Preparation of thin films with densely aggregated zinc phthalocyanine nanowires oriented uniaxially on friction-transferred polytetrafluoroethylene template

Chiyonobu, Yuki ; Koshiba, Yasuko ; Tomosada, Kana ; Matsumoto, Takuya ; Horike, Shohei ; Nishino, Takashi ; Ishida, Kenji ; Funahashi,…

(Citation)
Discover Polymers,2(1):8

(Issue Date)
2025-04-16

(Resource Type)
journal article

(Version)
Version of Record

Discover Polymers

Research

Preparation of thin films with densely aggregated zinc phthalocyanine nanowires oriented uniaxially on friction-transferred polytetrafluoroethylene template

Yuki Chiyonobu[1] · Yasuko Koshiba[1,2] · Kana Tomosada[1] · Takuya Matsumoto[1] · Shohei Horike[1,2,3] · Takashi Nishino[1] · Kenji Ishida[4] · Masahiro Funahashi[1,2]

Received: 31 October 2024 / Accepted: 3 April 2025
Published online: 16 April 2025

Abstract
One-dimensional nanostructures of organic semiconductors exhibit distinctive optical and electrical properties. In this study, thin films containing densely aggregated, uniaxially oriented zinc phthalocyanine (ZnPc) nanowires are fabricated through vapor deposition on polytetrafluoroethylene (PTFE) friction-transferred films as orientation-inducing templates. The aggregation behavior of the ZnPc molecules depends on the substrate temperature (T_s) during deposition and the film thickness. Full-coverage aggregated ZnPc nanowires aligned parallel to the friction direction are formed in a film with a thickness of 20 nm deposited at $T_s = 120$ °C. Within the ZnPc nanowires, α-ZnPc crystals are aligned with the b-axis along the direction of nanowire growth and the a-axis perpendicular to the substrate. This indicates that the longitudinal direction of the ZnPc nanowires corresponds to the π−π stacking direction of ZnPc molecules. A model detailing the growth of ZnPc nanowires on a PTFE film is proposed, elucidating the crystal growth and orientation through graphoepitaxial and epitaxial-like mechanisms. The PTFE friction-transferred film is demonstrated to be an effective template for the growth of aligned ZnPc nanowires. The uniaxially oriented, full-coverage ZnPc nanowire thin film fabricated on the PTFE template showed anisotropic electrical properties.

1 Introduction

Dimensionally−controlled nanostructures composed of organic semiconductors can perform functions that are not achievable in their bulk state [1]. Among these, one-dimensional (1D) nanostructures, such as nanowires, nanorods, and nanopillars, are anticipated to exhibit anisotropic optical and electrical properties and can be utilized as an active layer in various optical and electronic devices [2, 3]. For example, nanowires composed of conjugated organic small molecules realize excellent charge transport along the long axis [4]. Therefore, in-plane uniaxially oriented organic semiconductor nanowires are promising structures for devices that function through in-plane uniaxial carrier transport, such as organic field-effect transistors (OFETs).

Supplementary Information The online version contains supplementary material available at https://doi.org/10.1007/s44347-025-00020-w.

✉ Yasuko Koshiba, koshiba@kobe-u.ac.jp; ✉ Masahiro Funahashi, funahashi.masahiro@phoenix.kobe-u.ac.jp | [1]Department of Chemical Science and Engineering, Graduate School of Engineering, Kobe University, 1 - 1 Rokkodai-cho, Kobe 657 - 8501, Japan. [2]Research Center for Membrane and Film Technology, Kobe University, 1 - 1 Rokkodai-cho, Kobe 657 - 8501, Japan. [3]Center for Environmental Management, Kobe University, 1 - 1 Rokkodai-cho, Kobe 657 - 8501, Japan. [4]Department of Applied Quantum Physics and Nuclear Engineering, Faculty of Engineering, Kyushu University, 744 Motooka, Fukuoka 819 - 0395, Japan.

Metal phthalocyanine is an organic semiconductor with extended π-conjugation on its molecular planes [5] and possesses desirable properties, including nontoxicity [6], superior thermal and chemical stability [7, 8], film formability [9], and excellent optical properties [10]. These materials find applications in electronic devices such as OFETs [11], organic solar cells [12], and gas sensors [13]. Phthalocyanine (Pc) molecules tend to aggregate along the stacking direction of their molecular planes, owing to π−π interactions, which is favorable for charge transport [14]. The 1D nanostructures of Pc molecules serve as promising building blocks for high-performance and highly integrated nanodevices. Various studies have reported methods for controlling the 1D nanostructures of Pc molecules, such as physical vapor deposition (PVD) [15, 16], solution processes [17], and vacuum deposition [18, 19]. In our previous studies, we produced 1D Pc nanostructures via vacuum deposition by carefully selecting the substrate material and controlling the substrate temperature (T_s) during the Pc deposition process [18, 20]. However, achieving in-plane uniaxially oriented Pc nanowires presents challenges; therefore, we investigated polytetrafluoroethylene (PTFE) friction-transferred films as templates for achieving in-plane orientation of the Pc nanowires. The friction transfer technique involves squeezing and sliding a polymer block or pellet against a heated substrate under pressure, forming a highly oriented polymer thin film on the substrate surface [21]. In 1991, Wittmann and Smith reported that PTFE films prepared through the friction transfer technique can be utilized to orient other materials [22]. Since then, these films have been used as orientation-inducing layers for various low-molecular-weight molecules [23, 24] and polymers [25, 26] in both vacuum [27] and solution-based methods [25]. Additionally, we utilized PTFE friction-transferred films to orient liquid-crystalline semiconductors [28, 29].

Here, we produced full-coverage aggregated Pc nanowires that were uniaxially aligned in thin films. These thin films, consisting of Pc nanowires, can serve as the active layer in thin-film devices. Several studies have detailed the fabrication of Pc nanowires through PVD or physical vapor transport (PVT) methods. Li et al. recently created phthalocyanine nanowires on friction-transferred films through PVD [23], while Liao et al. fabricated aligned Pc nanowires on a sapphire surface with hydrophobic nanogrooves treated by PDMS gel using the PVT method [30]. Both the PVD and PVT methods offer simple experimental setups for producing nanowires. However, the Pc nanowires fabricated using PVD or PVT were not full-coverage aligned Pc nanowires, and they were not realized in a thin film state. Full-coverage aligned Pc nanowire thin films are more desirable for use as active layers in thin-film devices.

In this study, we fabricated thin films with uniaxially oriented Pc nanowires to achieve full-coverage aggregation in a thin film state on PTFE friction-transferred films using the vapor deposition method while controlling the deposition conditions, such as substrate temperature (T_s) and film thickness. In this experiment, zinc phthalocyanine (ZnPc), a Pc material with a central Zn metal known for its high carrier mobility [31], was utilized. The morphology, absorption spectrum, and X-ray diffraction (XRD) were examined as structural characterizations of the ZnPc thin films prepared under various conditions to determine the optimal fabrication conditions for the ZnPc nanowire thin film. Based on these structural evaluations, we propose a growth model for uniaxially oriented ZnPc nanowires considering the morphology of PTFE friction-transferred films. The model also considers the crystalline structures of both PTFE films and ZnPc nanowires, explaining the growth in terms of graphoepitaxial and epitaxial growth mechanisms. Finally, the electrical anisotropy of uniaxially oriented ZnPc nanowires was examined.

2 Material and methods

2.1 Material

Vacuum-sublimated ZnPc (purity: 98.0%) was purchased from Tokyo Chemical Industries and the chemical structure of ZnPc is shown in Fig. 1a. Molybdenum (XI) oxide (MoO_3, purity: 99.99%) was purchased from Sigma-Aldrich. All chemical materials were used as received.

2.2 Preparation of PTFE friction-transferred films and ZnPc thin films

The PTFE blocks utilized for friction transfer were prepared by cutting a 3-mm-thick commercial PTFE plate into 10-mm-wide pieces. PTFE thin films were fabricated on glass, quartz glass, and silicon substrates through a friction transfer technique using a hot-melt coating machine (Imoto IMC- 115 A). The friction transfer process was conducted in the air by pressing and sliding the PTFE block on substrates maintained at 150 °C. The pressure applied during pressing was 4.9×10^5 Pa, and the drawing speed was 60 mm/min. A diagram of the friction transfer method is presented in Fig. 1b.

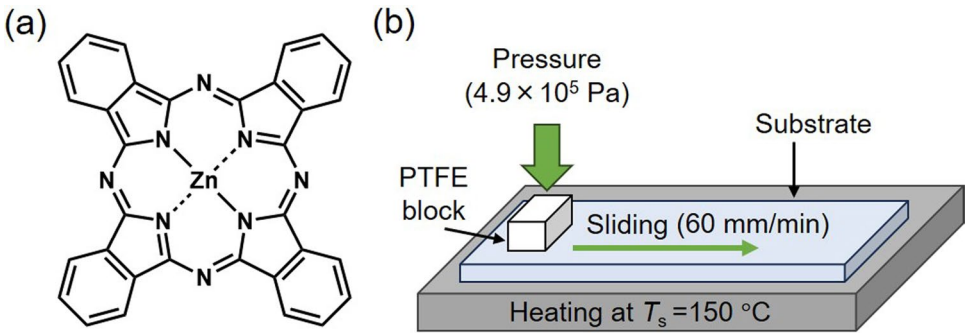

Fig. 1 **a** Chemical structure of ZnPc and **b** schematic of friction transfer technique

ZnPc thin films were deposited onto quartz glass (quartz), Si substrates (Si), and quartz and Si substrates on which PTFE was friction-transferred (quartz/PTFE and Si/PTFE) under vacuum conditions ranging from 1×10^{-4} to 5×10^{-4} Pa. The substrate temperatures (T_s) were room temperature (RT), 100, 120, 150, and 180 °C, and the deposition rate varied from 0.01 to 0.03 nm/s. The deposition rate and film thickness were monitored using a quartz crystal microbalance (QCM) in the chamber, while the substrate temperature (T_s) was measured using a thermocouple attached to the substrates. Subsequently, 3-nm-thick MoO_3 films were deposited on ZnPc thin films at varied deposition rates of 0.01–0.03 nm/s, and 80-nm-thick Au electrodes were deposited at varied deposition rates of 0.03–0.05 nm/s. MoO_3 and Au electrodes were formed using a shadow mask for patterning the electrodes.

2.3 Characterization of ZnPc thin films

The morphologies of PTFE friction-transferred and ZnPc thin films were examined using atomic force microscopy (AFM) (JEOL JSPM-5200 & HITACHI SPA400) and field-emission scanning electron microscopy (FE-SEM) (JEOL JSM-7500 F & JSM-IT800). The optical properties of the ZnPc thin films were analyzed using ultraviolet–visible–near infrared (UV–vis–NIR) spectrophotometry (JASCO V-670 & V-770), UV–vis spectrophotometry (JASCO V-750), and Fourier transform infrared (FT-IR) spectroscopy (JASCO FT/IR-600 Plus, FT/IR-600). Out-of-plane and in-plane XRD patterns were measured using a Rigaku Ultima IV Protectus and a Rigaku Smart Lab®, respectively. CuKα radiation (λ = 1.5418 Å) was used for both out-of-plane and in-plane XRD. All electrical characterizations were measured using a B2902 A Precision Source/Measure Unit at a substrate temperature (T_s) of 25 °C and atmospheric pressure. The resistance (R) of the ZnPc nanowire thin film was determined from the slope of the plot of the current as a function of the applied voltage based on the Ohmic law. The conductivity (σ) of the ZnPc nanowire thin film was derived from R, using Eq. 1:

$$\sigma = \frac{1}{R} \times \frac{l}{wt} \tag{1}$$

where w is the width of channel, l is the distance between electrodes, and t is the film thickness. The values of w and l were measured after the electrodes were formed and QCM thickness was used for t.

3 Results and discussion

3.1 Structure of PTFE friction-transferred films

AFM images, line profiles, and three-dimensional (3D) images of PTFE friction-transferred films prepared on glass and Si substrates are depicted in Fig. 2a and b. The line profiles reveal the roughness along the red arrows in the AFM images. An SEM image of the PTFE friction-transferred film on the Si substrate is presented in Fig. 2c. Striped structures were observed along the drawing direction of the PTFE block on both glass and Si substrates. Analysis of the line profiles and 3D images revealed that the depth of grooves was approximately 10 nm, while the width of the grooves in the striped structure varied from 40 to 80 nm on both glass and Si substrates.

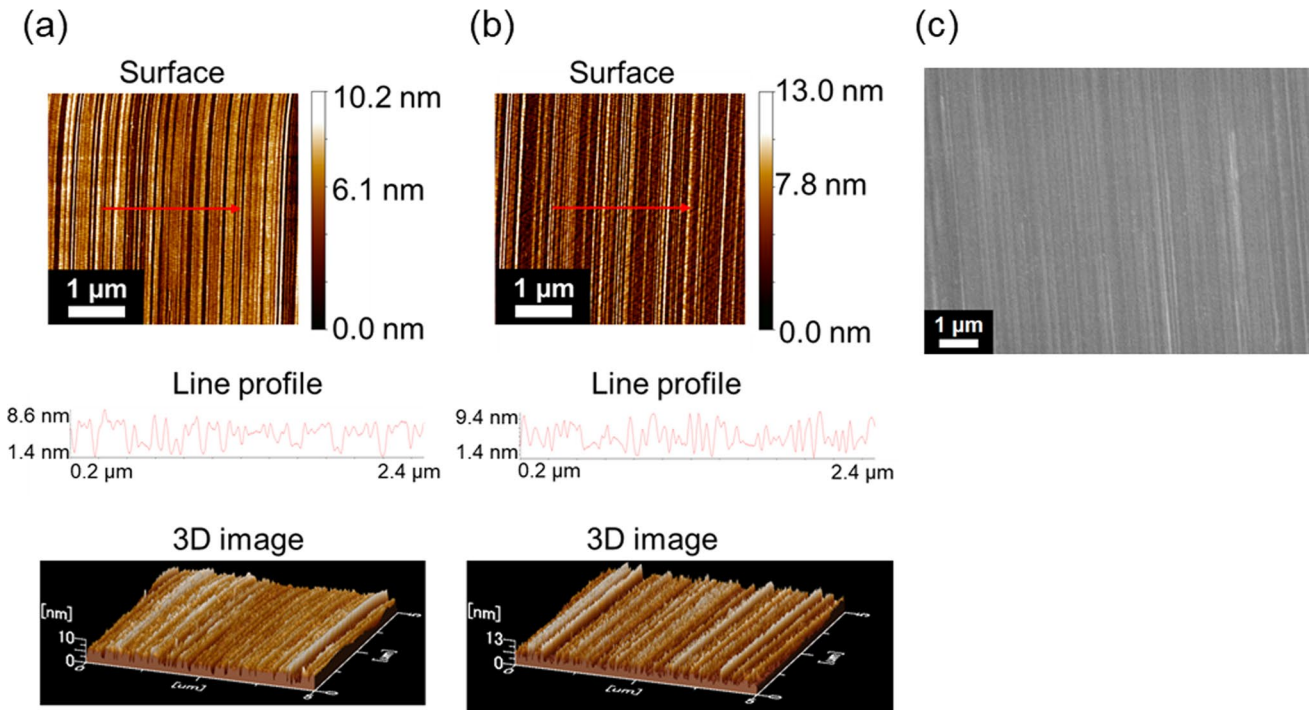

Fig. 2 **a**, **b** AFM images (top), line profiles (sections at red arrows in AFM images) (middle), and 3D images (bottom) of PTFE friction-transferred films fabricated on **a** glass substrate and **b** Si substrate. **c** SEM image of the PTFE friction-transferred films fabricated on Si substrate

3.2 Substrate temperature (T_s) dependence of ZnPc thin film morphology

The surface morphologies (SEM and AFM images) of 50 nm ZnPc thin films fabricated on Si and Si/PTFE substrates at T_s = RT are shown in Fig. 3a and b, respectively. The ZnPc thin film on the Si substrate consisted of small particles with diameters ranging from 20 to 40 nm (Fig. 3a). On Si/PTFE, particles measuring 20−70 nm were observed, exhibiting a

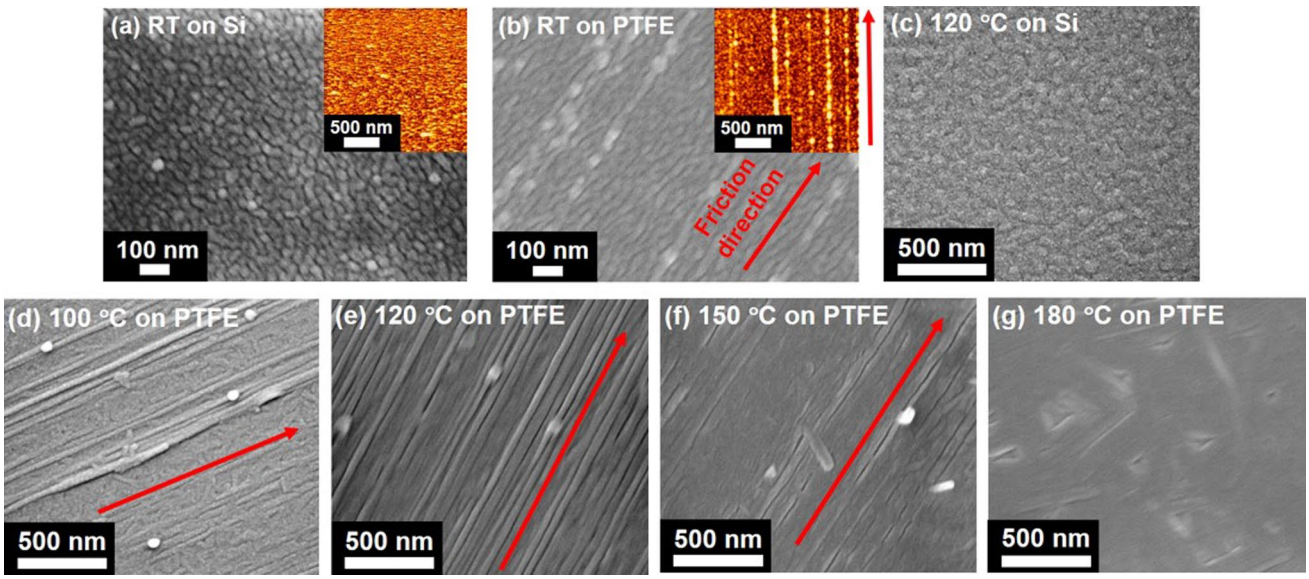

Fig. 3 SEM and AFM (inset) images of ZnPc thin films deposited on **a** Si substrate at T_s = RT and **b** Si/PTFE substrate at T_s = RT. SEM images of ZnPc thin films deposited on **c** Si at T_s = 120 °C, **d** Si/PTFE at T_s = 100 °C, **e** Si/PTFE at T_s = 120 °C, **f** Si/PTFE at T_s = 150 °C, and **g** Si/PTFE at T_s = 180 °C. Red arrows indicate the direction of friction transfer

slight alignment similar to the striped structure of the PTFE friction-transferred films. Some particles were larger than those on Si due to the low surface free energy of PTFE, facilitating the likelihood of molecular diffusion and aggregation on the substrates [23, 32].

Figure 3c shows an SEM image of a 20 nm ZnPc thin film fabricated on a Si substrate at T_s = 120 °C. Figure 3d–g exhibit SEM images of 20 nm ZnPc thin films fabricated on Si/PTFE at T_s = 100, 120, 150, and 180 °C, respectively. In the Si/ZnPc thin film at T_s = 120 °C (Fig. 3c), the particle size ranged from 60 to 90 nm, larger than the particle sizes of that at T_s = RT (Fig. 3a). Generally, vapor-deposited thin films form through the nucleation and growth of molecules reaching the substrate in the vapor phase [33]. As the substrate temperature (T_s) increases, the kinetic energy of the molecules reaching the substrates increases, promoting the aggregation of ZnPc molecules through π−π interactions [32–34]. Consequently, it is considered that the particles in the Si/ZnPc thin film deposited at T_s = 120 °C (Fig. 3c) are larger and dispersed in-plane compared to those in the Si/ZnPc thin film deposited at T_s = RT (Fig. 3a).

On the heated Si/PTFE substrate, the morphology of the ZnPc thin films underwent significant changes. At T_s = 100 °C (Fig. 3d), nanowires measuring 25−40 nm in width grew to several micrometers, but oriented nanowires were partially formed, and crystals grew randomly in some areas. At T_s = 120 °C (Fig. 3e), nanowires with a width of 30−50 nm and a length of several micrometers aligned uniaxially along the friction direction of the PTFE film in many regions. At T_s = 150 °C (Fig. 3f), most nanowires, with a width of 50−80 nm, aligned uniaxially similar to those at T_s = 120 °C, although some nanowires grew in other directions. Additionally, the boundaries between nanowires were not well defined in some regions, indicating coalescence of adjacent nanowires growing across the width direction or crystal growth in directions other than the PTFE grooves. Upon the deposition of ZnPc molecules on the PTFE friction-transferred films, the low surface energy of PTFE reduces the interaction of the film with ZnPc molecules, leading to a higher tendency for aggregation due to π−π interactions among ZnPc molecules [23, 32]. Upon deposition at T_s = RT, the particles aligned along the groove structure of PTFE (Fig. 3b); however, with increasing T_s, π−π interactions promoted molecular stacking and growth into wire-like crystals on the PTFE surfaces (Fig. 2d–f). At T_s = 180 °C (Fig. 3g), the formation of uniaxially oriented nanowires became challenging due to the perturbation caused by the random growth of nanocrystals. Uniaxially oriented nanowires were successfully fabricated on the PTFE friction-transferred films at T_s = 120 °C.

3.3 UV–vis spectra of ZnPc thin films

ZnPc thin films primarily exist in the metastable α-form or stable β-form, as shown in Fig. 4a. Both polymorphs exhibit distinct absorption spectra [35]. To analyze the crystal forms of the thin films, we measured the UV–vis spectra of ZnPc thin

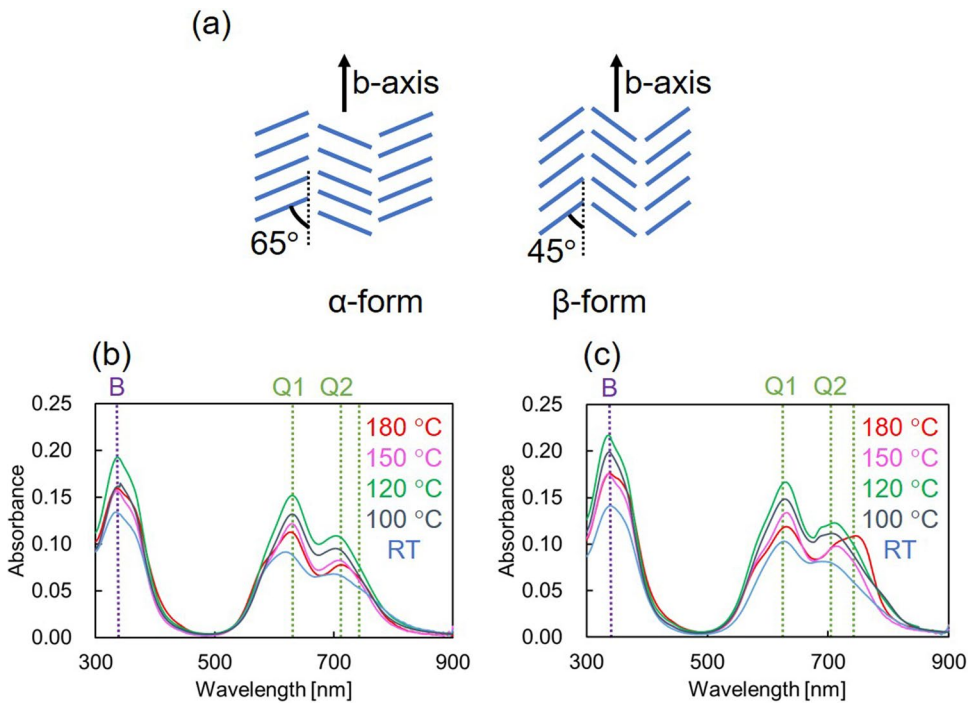

Fig. 4 **a** Schematics of molecular packing of α-form and β-form ZnPc. UV–vis spectra of **b** quartz/ZnPc and **c** quartz/PTFE/ZnPc thin films deposited at T_s = RT, 100, 120, 150, 180 °C

films fabricated at different substrate temperatures (T_s). Figure 4b and c show the UV–vis spectra of 20 nm ZnPc thin films deposited on quartz and quartz/PTFE at T_s = RT, 100, 120, 150, and 180 °C. The absorption peak at around 340 nm, known as the B-band, corresponds to the π-π* transition involving an electron transition from a_{1u} to e_g. The absorption band at 550—800 nm, referred to as the Q-band, corresponds to the π-π* transition with an electron transition from b_{2u} to e_g [36]. Owing to Davydov splitting, the Q-band absorption manifests as a doublet peak [37], with Q1 representing the lower wavenumber peak and Q2 the high wavenumber peak. The band gap energy of ZnPc has been reported to be 1.8 eV and ZnPc is generally known to be a p-type semiconductor [38, 39]. Jungyoon et al. reported that in the α-form, Q1 exhibits higher absorbance than Q2, while Q2 becomes predominant after thermal annealing, signifying a phase transition to the β-form. They also observed a red shift in both peaks [40]. In the quartz/ZnPc thin films (Fig. 4b), annealing below 180 °C favored the α-form, evident from the higher absorbance in Q1 compared to Q2. The presence of a shoulder at 740 nm in Q2 at 180 °C indicates an increasing proportion of the β-form. In the quartz/PTFE/ZnPc thin films (Fig. 4c), the α-form predominated at T_s = RT, 100, 120, and 150 °C, while a red-sift to 745 nm was observed in Q2 at 180 °C, with a shoulder around 710 nm. Additionally, the absorbance ratio of Q2 to Q1 increased compared to the spectrum below T_s = 150 °C. These trends are characteristics of quartz/PTFE/ZnPc films, suggesting that deposition on PTFE friction-transferred films may promote the formation of the β-form. Given that the α-form of ZnPc exhibits superior conductivity [41], it is deemed more suitable for device applications compared to the β-form. The T_s-dependent morphology and UV–visible spectra of the thin films indicate that depositing ZnPc at T_s = 120 °C on PTFE friction-transferred films results in the formation of uniaxially oriented nanowires predominantly in the α-form.

3.4 Dependence of ZnPc thin film morphology on film thickness

We investigated the morphological variations concerning the film thickness of the deposited ZnPc thin films on Si/PTFE substrate at T_s = 120 °C, which was identified as the optimal temperature for ZnPc nanowire formation. Figure 5a—d show the SEM images of ZnPc thin films fabricated at T_s = 120 °C with QCM film thicknesses of 5, 20, 30, and 50 nm on the Si/PTFE substrates. In the 5 nm thin film (Fig. 5a), a discontinuous wire-shaped morphology with a width of 10—20 nm and a length of several hundred nanometers was observed along the friction direction. This phase is considered to be the

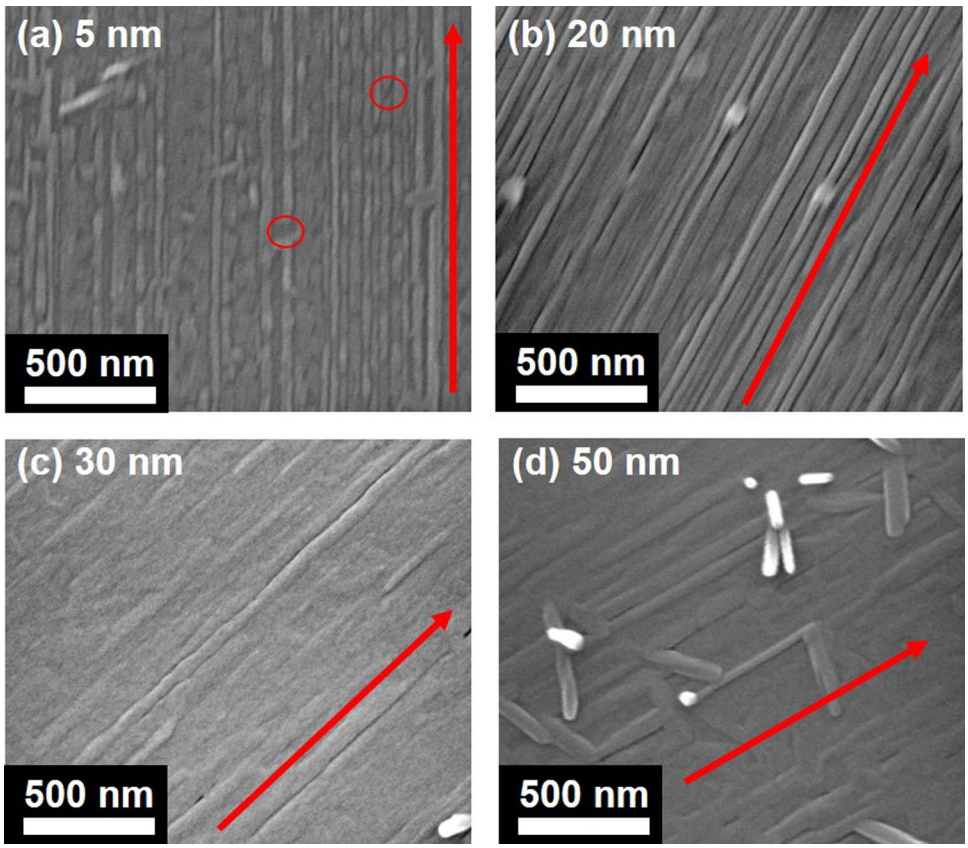

Fig. 5 SEM images of Si/PTFE/ZnPc thin films deposited at T_s = 120 °C with film thicknesses of **a** 5 nm, **b** 20 nm, **c** 30 nm, **d** 50 nm

initial stage of crystal growth due to the presence of non-continuous nanowires, as indicated by sections surrounded by red circles. At 20 nm (Fig. 5b), highly uniaxially oriented nanowires extended further along the friction direction. A larger area of the same thin film in Fig. 5b is shown in the SEM image in Fig. S1, showing densely aligned nanowires that covered a wide area. The nanowires had a width of 30—50 nm and reached a maximum length of approximately 3.5 µm. Even at 30 nm (Fig. 5c), a wire-shaped morphology persisted along the friction direction, with nanowire widths expanding to 40—70 nm and the coalescence of adjacent nanowires growing in the width direction. In the case of 50 nm (Fig. 5d), the uniaxial growth of nanowires was confirmed, although some nanowires exhibited random growth patterns without alignment in a single direction. Cross-sectional SEM images of the Si/PTFE/ZnPc thin films deposited at T_s = 120 °C are shown in Fig. S2 (a) and (b). In the 20-nm-thick Si/PTFE/ZnPc thin film, the nanowires ranged in height from 10 to 40 nm, and no out-of-plane growth of the ZnPc nanowires was observed, indicating solely in-plane nanowire growth (Fig. S2 (a)). However, in the 50-nm-thick Si/PTFE/ZnPc thin film, out-of-plane growth of the ZnPc nanowires was evident (Fig. S2 (b)).

During ZnPc deposition on the PTFE friction-transferred films at T_s = 120 °C, nanowires formed and aligned along the friction direction from the initial stage. Uniaxially oriented nanowires were formed with a QCM film thickness of approximately 20 nm. Beyond this thickness, non-uniform growth of ZnPc nanowires in the in-plane direction was observed. Further increasing the film thickness to 50 nm, resulted in growth in the out-of-plane direction. These findings suggest that the deposition of ZnPc on the PTFE friction-transferred films with a 20 nm thickness at T_s = 120 °C is suitable to produce full-coverage, uniaxially oriented ZnPc nanowires.

3.5 Out-of-plane orientation of ZnPc molecules in thin films

The out-of-plane molecular orientation of ZnPc in the thin films was analyzed using transmission FT-IR spectroscopy. Figure 6a shows the transmission IR spectra of ZnPc powder in a KBr pellet and ZnPc thin films on the Si and Si/PTFE substrates at T_s = 120 °C and a thickness of 20 nm. Molecular vibrations were strongly detected in the in-plane direction of the substrate, while those in the out-of-plane direction were difficult to detect [10]. The spectrum of ZnPc powder in Fig. 6a (i) reveals absorption peaks corresponding to the Pc backbone between 700 and 1200 cm^{-1}. The absorption bands at 726 and 775 cm^{-1} are attributed to the out-of-plane C-H deformation mode. Additionally, the absorption bands at 755, 1060, 1090, 1118, and 1165 cm^{-1} correspond to the C-H in-plane bending mode [10, 35]. Specially, the focus was on the out-of-plane (perpendicular to the molecular plane) C-H deformation mode at 726 cm^{-1} and the in-plane (parallel to the molecular plane) C-H bending mode at 1118 cm^{-1}. The transmission FT-IR spectra of Si/ZnPc and Si/PTFE/ZnPc thin films are presented in Fig. 6a (ii) and (iii). Absorption peaks at 726 and 1118 cm^{-1} were clearly observed in the ZnPc powder spectrum. However, in the transmission spectra of Si/ZnPc and Si/PTFE/ZnPc thin films, strong peaks for the out-of-plane C-H bending mode were observed at 720 cm^{-1}, while small absorption peaks for the in-plane C-H bending mode were observed at 1118 cm^{-1}. These results indicate that ZnPc molecules are adsorbed obliquely with an edge-on orientation in both the Si/ZnPc and Si/PTFE/ZnPc thin films.

We conducted out-of-plane XRD measurements to analyze the out-of-plane crystalline structures of the ZnPc thin films. The XRD patterns of the Si/ZnPc and Si/PTFE/ZnPc thin films deposited at T_s = 120 °C and 20 nm-thick are shown in Fig. 6b. A diffraction peak was observed at 2θ = 7.03° in the Si/ZnPc thin film and at 2θ = 6.95° in the Si/PTFE/ZnPc thin film. The lattice spacing was calculated as d = 1.257 nm for the Si/ZnPc thin film and d = 1.271 nm for the Si/PTFE/

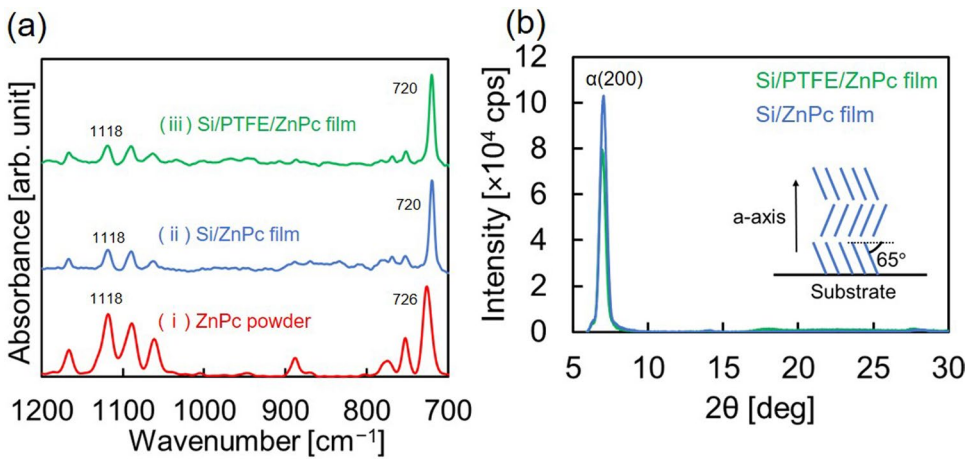

Fig. 6 **a** Transmission FT-IR spectrum of ZnPc powder in KBr pellets, Si/ZnPc and Si/PTFE/ZnPc thin films deposited at T_s = 120 °C, with a thickness of 20 nm. **b** Out-of-plane XRD patterns of Si/ZnPc and Si/PTFE/ZnPc thin films deposited at T_s = 120 °C and with a thickness of 20 nm. The inset shows the schematic of the a-axis direction against the substrate and out-of-plane molecular orientation

ZnPc thin film. This diffraction peak was assigned to the (200) plane of the monoclinic α-ZnPc phase [42], indicating that the a-axis of the unit cell was perpendicular to the substrate. Transmission FT-IR spectra and out-of-plane XRD patterns revealed that ZnPc molecules formed α-form crystals with the a-axis oriented perpendicular to the substrates. The molecules exhibit an edge-on orientation in ZnPc nanowire thin films because ZnPc molecules lean around 65° against the b-axis in the unit cell [35, 43].

3.6 Polarized absorption spectroscopy

Polarized UV–vis absorption measurements were conducted, and the measurement setup is depicted schematically in Fig. 7a. In the case of the quartz/PTFE/ZnPc thin film, the friction direction corresponds to the longitudinal direction of uniaxially oriented nanowires, and the configuration in which the friction direction and polarization were parallel was labeled as 0°. UV–vis spectra were collected by incrementally rotating the quartz/PTFE/ZnPc thin film in 10° until the friction and polarization directions were perpendicular (90°). For the quartz/ZnPc thin film, an arbitrary direction was defined as 0°, and the spectrum was recorded from 0° to 90° in 10° increments by rotating the film.

Figure 7b and c show the polarized UV–vis absorption spectra of 20-nm-thick ZnPc thin films deposited at T_s = 120 °C on the quartz and quartz/PTFE substrates, respectively. Both thin films exhibit a B-band around 340 nm and a Q-band at 550—800 nm. For the quartz/ZnPc thin film (Fig. 7b), absorbance remains consistent across all polarization directions from 0° to 90°. Conversely, in the quartz/PTFE/ZnPc thin film, absorbance increases with the change in polarization direction from 0° to 90°. The dichroic ratio ($DR = A_{90°}/A_{0°}$) [44] was calculated as 0.97 for quartz/ZnPc and 1.26 for quartz/PTFE/ZnPc thin film based on Q1 absorbance at 0° and 90°. There have been reports of optical polarization of nanomaterial thin films [45–47]. However, the polarized UV–vis spectra of the PTFE friction-transferred films, which are nanostructured templates, showed no optical absorption without anisotropy in the UV region (Fig. S3). Therefore, the difference of absorbance depending on polarization direction of the quartz/PTFE/ZnPc thin film is due to the orientation of the ZnPc

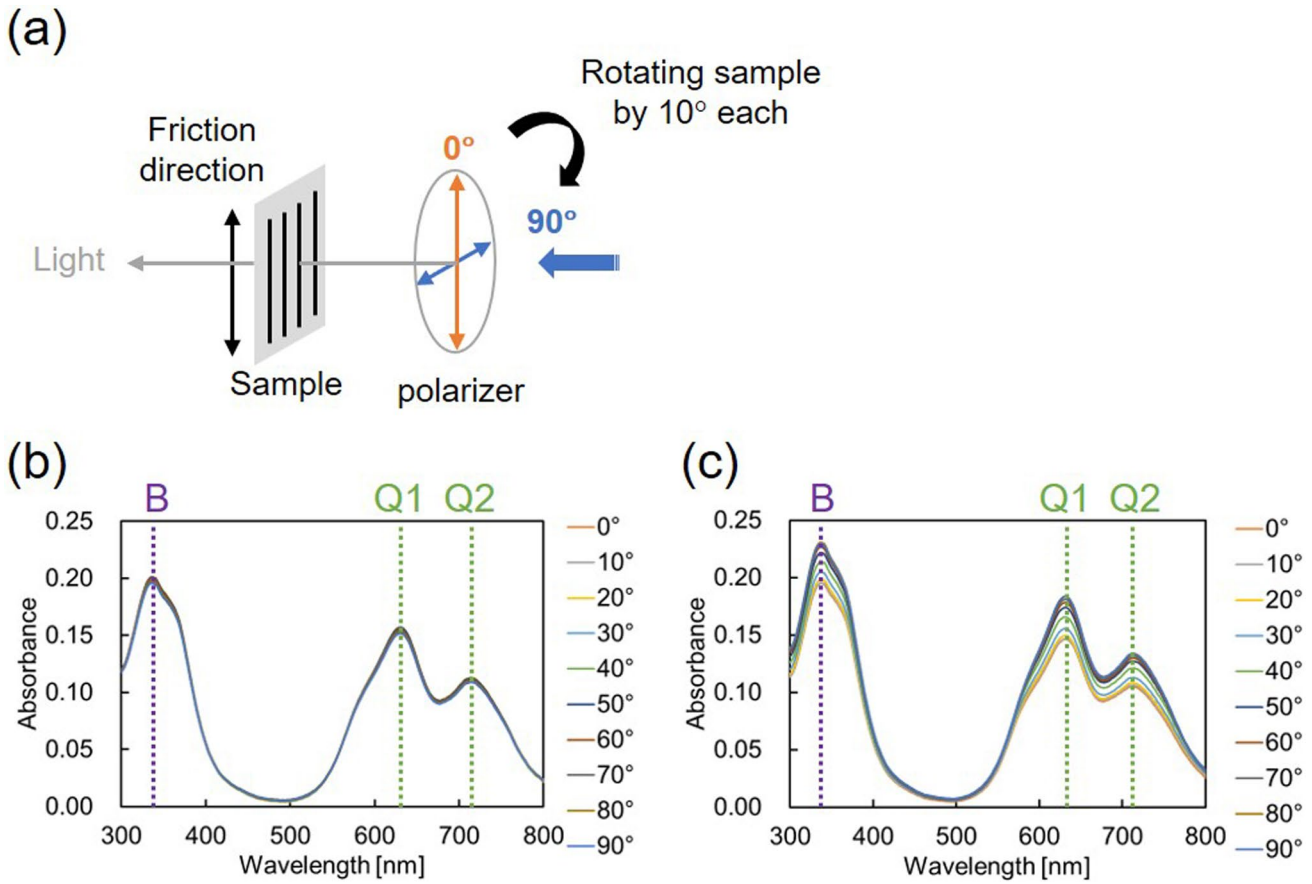

Fig. 7 **a** Schematic of polarized UV–vis measurement of quartz/PTFE/ZnPc thin film. Polarized UV–vis spectra from 0° to 90° of **b** quartz/ZnPc and **c** quartz/PTFE/ZnPc thin films deposited at T_s = 120 °C and with a thickness of 20 nm

molecules in uniaxial alignment of ZnPc nanowires. In the quartz/ZnPc thin film, the transition dipole moments of ZnPc molecules were misaligned, indicating a lack of in-plane orientation. In contrast, the quartz/PTFE/ZnPc thin film exhibited a maximum absorbance at 90°, indicating that the transition dipole moment aligns perpendicular to the friction direction within the plane of the substrate. This alignment suggests that the ZnPc molecules are aligned with their molecular planes perpendicular to the friction direction owing to their in-plane transition dipole moments [48]. The FT-IR spectra and out-of-plane XRD patterns revealed that the ZnPc molecules adopt an edge-on orientation and were adsorbed to the substrates, leaning at an angle of approximately 65° against the substrate surface. Consequently, absorption occurs even at 0°, resulting in a *DR* as low as 1.26.

3.7 Characterization of in-plane orientation of ZnPc thin film

We conducted in-plane XRD ($2\theta\chi/\varphi$ scan) measurements to analyze the in-plane molecular orientation. A diagram of the measurement setup is illustrated in Fig. 8a. The incident X-ray is nearly parallel to the diffracted X-ray, while the detector rotates along the $2\theta\chi$ direction, and the sample rotates around the φ axis during the measurement [49]. The incident angle remained constant at 0.22° throughout the scan. In this experiment, we measured diffraction from lattice planes parallel and perpendicular to the friction direction for the Si/PTFE/ZnPc thin film, as shown in Fig. 8b. For the Si/ZnPc thin film, diffraction was measured from arbitrary directions and perpendicular to them.

The in-plane XRD patterns of 20-nm-thick Si/ZnPc or Si/PTFE/ZnPc thin films deposited at T_s = 120 °C are shown in Fig. 8c. The XRD patterns of the Si/ZnPc thin film are shown by red and blue lines, while those of the Si/PTFE/ZnPc thin film are indicated by green (parallel to the friction direction) and orange (perpendicular to the friction direction) lines. A diffraction peak at 2θ = 7.08° was observed in all patterns, corresponding to the (002) plane of α-ZnPc [50] with a lattice spacing of d = 1.249 nm. The diffraction intensity of this peak is similar in both directions for the Si/ZnPc thin film. In contrast, the intensity in the direction parallel to the friction direction was significantly higher than that perpendicular to the friction direction in the Si/PTFE/ZnPc thin film (Fig. 8c). These findings suggest that an unoriented structure was formed on the Si/ZnPc thin film, while the (002) planes were aligned along the friction direction, indicating an oriented structure in the ZnPc nanowire thin film deposited on the PTFE friction-transferred film. Analysis of the out-of-plane and in-plane XRD patterns suggests that a unit cell of α-ZnPc should be positioned as shown in Fig. 8d on the PTFE friction-transferred films. The (200) plane (purple plane) is parallel to the substrate, and the (002) plane (yellow plane) is parallel

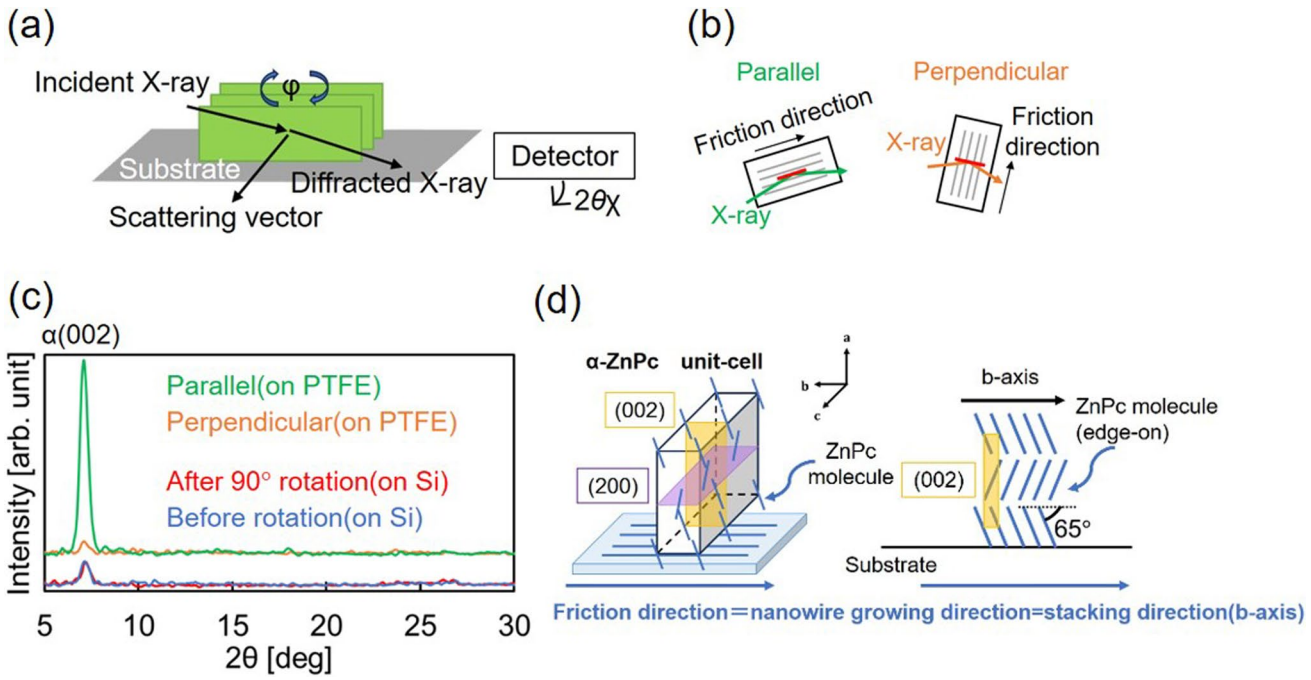

Fig. 8 **a** Schematic of in-plane XRD ($2\theta\chi/\varphi$ scan) setup. **b** Diffracted lattice planes (represented by red lines) on PTFE friction-transferred films. **c** In-plane XRD patterns of 20-nm-thick Si/ZnPc and Si/PTFE/ZnPc thin films deposited at T_s = 120 °C. **d** Schematics of ZnPc crystalline orientation on PTFE friction-transferred film

to the friction direction. According to this model, the ZnPc molecules were stacked along the b-axis, corresponding to the friction direction, maintaining an edge-on orientation against the substrates, and the nanowires grew in that direction. This model demonstrates that anisotropic growth of nanowires was achieved on the structural induction templates.

Figure S4 shows the in-plane XRD patterns of the 20-nm-thick Si/ZnPc and Si/PTFE/ZnPc thin films deposited at T_s = 150 °C. In the parallel direction of the Si/PTFE/ZnPc thin film deposited at T_s = 150 °C, a diffraction peak from the (002) plane is present in addition to a peak at 2θ = 9.16°. Shahiduzzaman et al. reported that the diffraction peak of the $(20\bar{1})$ plane appeared at 2θ = 9.3° in out-of-plane XRD results for a polymorph of ZnPc transited to a β-form [51]. Therefore, the diffraction peak at 2θ = 9.16° was considered to the $(20\bar{1})$ plane of a monoclinic β-ZnPc phase, indicating that the b-axis of the unit cell was oriented along the friction direction. This diffraction peak was observed in the PTFE transferred films and did not appear in the Si/ZnPc thin film. These results suggest increasing T_s and depositing films on PTFE friction-transferred films resulted in the increase of the β-form in the nanowire thin films. In addition, these results indicate that T_s = 120 °C is suitable for fabricating uniaxially oriented nanowires because the β-form exhibits inferior conductivity compared to the α-form.

3.8 ZnPc nanowire growth model on the PTFE friction-transferred films

Based on the experimental results, we propose a mechanism of ZnPc nanowire growth on the PTFE friction-transferred films. Uniaxially oriented ZnPc nanowire growth at T_s = 120 °C is illustrated in Fig. 9. ZnPc molecules reaching the substrate in the vapor phase diffuse to the interfaces between the PTFE and the substrate, where the surface free energy is relatively high, leading to nucleation of ZnPc molecules. The low surface energy of PTFE promotes the diffusion of ZnPc molecules on its surface. As mentioned in Sect. 3.2, at higher T_s, the kinetic energy of the ZnPc molecules increases, resulting in a decrease of nucleation on the PTFE friction-transferred films. Following nucleation, ZnPc molecules align along the molecular chain of PTFE through π—π interactions, initiating growth in the nanowire morphology. These phases occur at a deposit thickness of 5 nm, representing the initial step of crystal growth (Fig. 9a). With the deposition of more ZnPc molecules, the nanowires grow due to the adsorption and diffusion of ZnPc molecules, forming uniaxially oriented nanowires. At a deposit thickness of 20 nm, uniaxially oriented ZnPc nanowires are observed on the PTFE friction-transferred films along the friction direction, corresponding to the b-axis of ZnPc (Fig. 9b). In the 20—30 nm deposit thickness range, the ZnPc nanowires grow in both width and length due to the adsorption and aggregation of ZnPc molecules and adjacent nanowires grow along the width direction and coalesce (Fig. 9b). As the number of adsorbed molecules increased and film thickness reached over 30 nm (Fig. 9c), nucleation of ZnPc crystals occurred on the nanowires [52], with molecules gathering and aggregating at these nuclei. In addition, collisions occurred between the nanowires growing in the plane along the friction direction, leading to random growth of ZnPc nanowires including out-of-plane direction. At film thickness of 30—50 nm, some ZnPc nanowires were observed along the friction direction, in addition to other nanowires growing along the out-of-plane direction (Fig. 9c). In-plane uniaxially oriented ZnPc nanowire thin films are fabricated by controlling the substrate temperature and deposition film thickness on the PTFE friction-transferred films. The PTFE friction-transferred films serve as a high-quality structural induction template for the deposition of ZnPc films. It should be noted that nanogrooves with a depth of only approximately 10 nm induce the graphoepitaxial growth of ZnPc.

On the PTFE friction-transferred films, molecular orientation primarily occurs through a graphoepitaxial mechanism. Ueda et al. reported that copper phthalocyanine molecules align via a graphoepitaxial mechanism on the PTFE

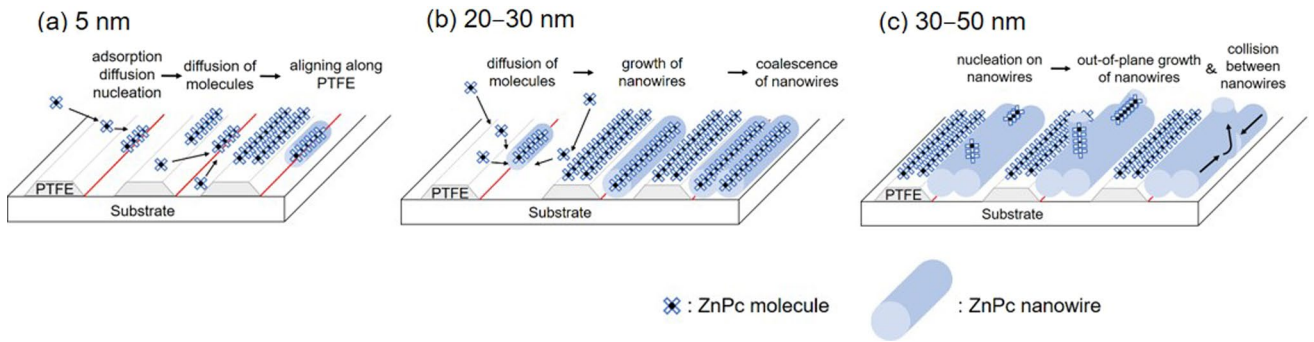

Fig. 9 Schematics of the models of nanowire growth on PTFE friction-transferred films: **a** initial phase (thickness = 5 nm), **b** middle phase (thickness = 20—30 nm), and **c** last phase (thickness = 30—50 nm)

friction-transferred films [53]. Here, we validate the potential of epitaxial growth in addition to graphoepitaxial growth. Generally, epitaxial growth is often encountered during crystal growth between inorganic – inorganic interfaces [54]. The epitaxial growth of organic thin films on inorganic substrates has also been reported [55]. Furthermore, epitaxial growth between organic – organic interfaces has been investigated, such as the growth of oligothiophene and hexa-*peri*-hexabenzocoronene (HBC) derivatives on PTFE friction-transferred films [56, 57]. Therefore, we focused on the lattice matching between ZnPc and PTFE. Ueda et al. reported that the c-axis (c = 19.50 Å) of the hexagonal PTFE phase aligns with the friction direction in PTFE friction-transferred films [53]. Additionally, we confirmed that the b-axis of monoclinic α-ZnPc (b = 3.78 Å) and monoclinic β-ZnPc (b = 4.85 Å) align with the friction direction [58]. The spacing of five unit cells of α-ZnPc is 18.90 Å, and that of four unit cells of β-ZnPc is 19.40 Å. Both spacings are close to the lattice spacing of the c-axis (19.50 Å) of PTFE, indicating favorable lattice matching in the growth direction of ZnPc nanowires, with β-ZnPc showing closer values than α-ZnPc. These results suggest that the lattice matching influences the formation of β-ZnPc on PTFE friction-transferred films at lower substrate temperatures (T_s) compared to Si or quartz substrates, despite the usual requirement for high-temperature annealing for transition to the β-form [40, 59]. In Fig. 4c, a red-shift of the Q2 peak in the UV–vis spectrum was observed for the quartz/PTFE/ZnPc thin film deposited at 180 °C. In Fig. S4, a diffraction peak of $(20\bar{1})$ of β-ZnPc was observed on the Si/PTFE/ZnPc thin film deposited at 150 °C. No β-ZnPc-derived peaks were observed in the spectra of ZnPc thin films deposited on quartz or Si substrates at the same T_s, indicating that the favorable lattice matching between β-ZnPc and PTFE may promote the growth of β-ZnPc crystals on the PTFE friction-transferred films. In the case of ZnPc nanowire growth on the PTFE friction-transferred films, molecular orientation is believed to occur not only through a graphoepitaxial mechanism but also through an epitaxial-like mechanism. PTFE friction-transferred films can induce oriented structures owing to their nanogroove morphology, low surface energy resulting from their hydrophobicity, and crystalline structure, facilitating both graphoepitaxial growth and epitaxial growth with lattice-matching.

We produced uniaxially oriented ZnPc nanowires that formed closely and continuously aggregated thin films, measuring 20 nm in thickness, on the PTFE friction-transferred films. Within the nanowires, ZnPc molecules adsorbed obliquely with an edge-on orientation, aligning their molecular planes perpendicular to the friction direction. Additionally, α-ZnPc crystals were oriented with the a-axis perpendicular to the substrate and the b-axis in the direction of nanowire growth.

3.9 Electrical characterizations of a ZnPc nanowire thin film

MoO_3 (3 nm)/Au (80 nm) electrodes [60, 61] were deposited on a 20-nm-thick ZnPc nanowire thin film fabricated at T_s = 120 °C, and *I* – *V* curves were measured to evaluate the anisotropic electrical properties of the uniaxially oriented thin film. The electrodes were positioned parallel and perpendicular to the friction direction on the ZnPc nanowire thin film (Fig. 10a). The *I* – *V* curves were measured along the long and short axis of the ZnPc nanowire for the parallel (Fig. 10a (1)) and perpendicular (Fig. 10a (2)) setups, respectively. The conductivity was calculated from the resistance results obtained via the slope of the *I* – *V* curves, distance between the electrodes, and the width of electrodes.

Figure 10b shows the current characteristics responded to the applied electric field (*E*) obtained from the *I* – *V* curves measured using the electrode pairs of (1) and (2). The green and orange lines show the current (*I*) – electric field (*E*) characteristics parallel and perpendicular to the friction direction, respectively. The curves are linear and demonstrate ohmic contact. The conductivities of the parallel and perpendicular directions were 5.68×10^{-5} and 1.48×10^{-5} S cm^{-1}, respectively. The conductivity along the parallel direction was approximately 3.8 times greater than that along the perpendicular direction, indicating superior electrical properties along the longitudinal direction of the ZnPc nanowires. The anisotropic electrical properties of the uniaxially oriented ZnPc nanowire thin films were revealed using a simple device structure.

4 Conclusions

In this study, the parameters involved in producing uniaxially oriented ZnPc nanowires on the PTFE friction-transferred films through vacuum deposition were investigated. By controlling the substrate temperature (T_s) and film thickness, we developed a model for the growth of ZnPc nanowires. ZnPc nanowires and molecular orientations were absent on substrates lacking PTFE friction-transferred films, which serve as templates for inducing orientation. On the PTFE friction-transferred films, ZnPc thin films deposited at T_s = RT consisted of particles, while ZnPc thin films deposited at

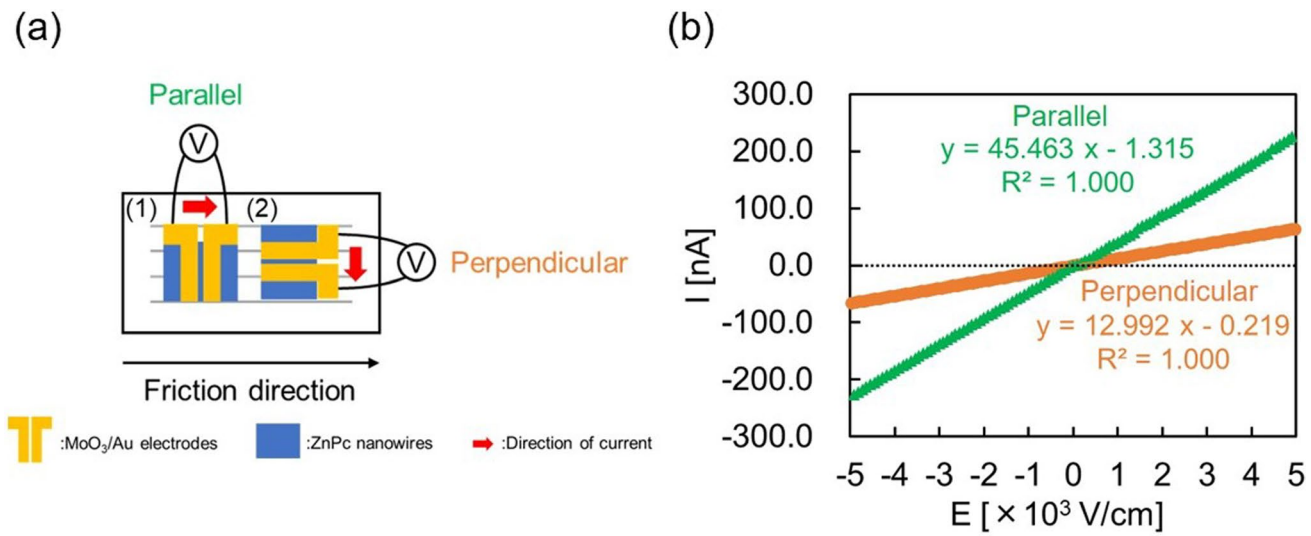

Fig. 10 **a** Schematic of the uniaxially oriented ZnPc nanowire device. **b** Current (*I*) characteristics in response to the electric field (*E*), which was applied parallel or perpendicular to the friction direction on the uniaxially oriented ZnPc nanowire thin film

T_s = 100−150 °C exhibited uniaxial nanowires aligned parallel to the friction direction. The temperature-dependent analysis of ZnPc thin film structure revealed that in the ZnPc nanowire thin films deposited at T_s = 120 °C, α-form crystals, known for their superior conductivity among ZnPc crystal polymorphs, were predominant. Additionally, the uniaxially oriented ZnPc nanowires extended over a large area. The dependence of the thin film structure on film thickness for films deposited at T_s = 120 °C indicated that the optimal film thickness for ZnPc nanowire formation is 20 nm. The ZnPc nanowires were closely aligned, resulting in a relatively homogeneous thin film. Upon structural evaluation of the ZnPc nanowire thin films produced under optimal conditions, we observed α-form crystals of ZnPc aligned with their a-axis perpendicular to the substrate and b-axis parallel to the friction direction. Thus, the π−π stacking direction, which is favorable for charge transport, was in the longitudinal direction of the ZnPc nanowires. We proposed a growth model of ZnPc nanowires on the PTFE friction-transferred films, considering both graphoepitaxial and epitaxial growth mechanisms. Our findings suggest that ZnPc crystal growth occurred not only though the graphoepitaxial mechanism but also through an epitaxial-like mechanism. The PTFE friction-transferred films serve as effective templates for inducing the molecular orientation and crystal growth of ZnPc, enabling the fabrication of thin films with full-coverage, aligned ZnPc nanowires in a planar configuration, which has been difficult to achieve in previous studies. The uniaxially oriented ZnPc nanowire thin films developed in this study exhibited anisotropic electrical properties.

In this study, the electrical properties were evaluated using a device with a simple structure, and further investigation of the device design is required. ZnPc nanowire thin films demonstrate the potential for application in various devices, including phototransistors and optical sensors.

Acknowledgements We thank Prof. Tatsuo Maruyama at Kobe University for his help with AFM measurements and Prof. Hideto Matsuyama at Kobe University for his assistance with FE-SEM measurements.

Author contributions Y.K. designed and conceived this study. Y.C. and Y.K. drafted the manuscript the supervision and guidance of S.H., K.I. and M.F. Y.C prepared thin films. Y.C and Y.K. performed measurement and characterization. K.T., T.M. and T.N. supported in-plane XRD measurements. The manuscript was written through contributions of all authors. All authors have given approval to the final version of the manuscript.

Funding This work was partially supported by the Kawanishi Memorial ShinMaywa Education Foundation.

Data availability The authors declare that the data supporting the findings of this study are available within the paper and its Supplementary Information files.

Declarations

Ethics approval and consent to participate Not applicable.

Consent for publication All the authors have read and agreed to the final copy of the finding as contained in the manuscript.

Competing interests The authors declare no competing interests.

References

1. Xia Y, Yang P, Sun Y, Wu Y, Mayers B, Gates B, Yin Y, Kim F, Yan H. One-dimensional nanostructures: synthesis, characterization, and applications- a review. Adv Mater. 2003;15:353–89. https://doi.org/10.1002/adma.200390087.
2. Zang L, Che Y, Moore JS. One-dimensional self-assembly of planar π-conjugated molecules: adaptable building blocks for organic nanodevices. Acc Chem Res. 2008;41:1596–608. https://doi.org/10.1021/ar800030w.
3. Min S-Y, Kim T-S, Lee Y, Cho H, Xu W, Lee T-W. Organic nanowire fabrication and device applications. Small. 2015;11:45–62. https://doi.org/10.1002/smll.201401487.
4. Briseno AL, Mannsfeld SCB, Jenekhe SA, Bao Z, Xia Y. Introducing organic nanowire transistors. Mater Today. 2008;11:38–47. https://doi.org/10.1016/S1369-7021(08)70055-5.
5. Suen S-C, Whang W-T, Hou F-J, Dai B-T. Low-temperature self-assembly of copper phthalocyanine nanofibers. Org Electron. 2006;7:428–34. https://doi.org/10.1016/j.orgel.2006.05.008.
6. Sathyamoorthy R, Senthilarasu S, Lalitha S, Subbarayan A, Natarajan K, Mathew X. Electrical conduction properties of flash evaporated ZincPhthalocyanine (ZnPc) thin films. Sol Energy Mater Sol Cells. 2004;82:169–77. https://doi.org/10.1016/j.solmat.2004.01.015.
7. Ribeiro AO, Biazzotto JC, Serra OA. A phthalocyanine covalently bonded to a silica network by a sol–gel process. J Non-Cryst Solids. 2000;273:198–202. https://doi.org/10.1016/S0022-3093(00)00130-7.
8. de la Torre G, Claessensa CG, Torres T. Phthalocyanines: old dyes, new materials. Putting color in nanotechnology. Chem Commun. 2007;20:2000–15. https://doi.org/10.1039/B614234F.
9. Senthilarasu S, Sathyamoorthy R, Lalitha S, Subbarayan A, Natarajan K. Thermally evaporated ZnPc thin films—band gap dependence on thickness. Sol Energy Mater Sol Cells. 2004;82:179–86. https://doi.org/10.1016/j.solmat.2004.01.016.
10. Zanfolim AA, Volpati D, Olivati CA, Job AE, Constantino CJL. Structural and electric-optical properties of zinc phthalocyanine evaporated thin films: temperature and thickness effects. J Phys Chem C. 2010;114:12290–9. https://doi.org/10.1021/jp1008913.
11. Li L, Tang Q, Li H, Hu W, Yang X, Shuai Z, Liu Y, Zhu D. Organic thin-film transistors of phthalocyanines. Pure Appl Chem. 2008;80:2231–40. https://doi.org/10.1351/pac200880112231.
12. Suzuki A, Ohtsuki T, Oku T, Akiyama T. Fabrication and characterization of tetracyanoquinodimethane/phthalocyanine solar cells. Mater Sci Eng B. 2012;177:877–81. https://doi.org/10.1016/j.mseb.2012.03.052.
13. Miyata T, Kawaguchi S, Ishii M, Minami T. High sensitivity chlorine gas sensors using Cu–phthalocyanine thin films. Thin Solid Films. 2003;425:255–9. https://doi.org/10.1016/S0040-6090(02)01129-X.
14. Wu Y, Zhang X, Pan H, Zhang X, Zhang Y, Zhang X, Jie J. Large-area aligned growth of single-crystalline organic nanowire arrays for high-performance photodetectors. Nanotechnology. 2013;24:35520. https://doi.org/10.1088/0957-4484/24/35/355201.
15. Mirabito T, Huet B, Redwing JM, Snyder DW. Influence of the underlying substrate on the physical vapor deposition of Zn-Phthalocyanine on graphene. ACS Omega. 2021;6:20598–610. https://doi.org/10.1021/acsomega.1c02758.
16. Wang F-X, Yuan G-H, Liu Y-D, Pan G-B. Synthesis and optoelectronic properties of helical nanowires of cobalt phthalocyanine. Mater Lett. 2012;83:56–8. https://doi.org/10.1016/j.matlet.2012.05.091.
17. Higashi T, Ohmori M, Ramananarivo MF, Fujii A, Ozaki M. Single crystal growth in spin-coated films of polymorphic phthalocyanine derivative under solvent vapor. APL Mater. 2015;3: 126107. https://doi.org/10.1063/1.4937169.
18. Koshiba Y, Sugimoto I, Horike S, Fukushima T, Ishida K. Fabrication and local electrical characterization of p–n junction copper phthalocyanine nanorods. Phys Status Solidi A. 2023;220:2300243. https://doi.org/10.1002/pssa.202300243.
19. Senthilarasu S, Hahn YB, Lee S-H. Nano structure formation in vacuum evaporated zinc phthalocyanine (ZnPc) thin films. J Mater Sci Mater Electron. 2008;19:482–6. https://doi.org/10.1007/s10854-007-9368-4.
20. Koshiba Y, Ohnishi T, Morimoto M, Misaki M, Fukushima T, Ishida K. Nanorod growth of copper phthalocyanine on fluorinated phosphonic acid SAM-modified indium tin oxide substrate for organic photovoltaic devices. Mol Cryst Liq Cryst. 2017;365:157–63. https://doi.org/10.1080/15421406.2017.1351280.
21. Breiby DW, Sølling TI, Bunk O, Nyberg RB, Norrman K, Nielsen MM. Structural surprises in friction-deposited films of Poly(tetrafluoroethylene). Macromolecules. 2005;38:2383–90. https://doi.org/10.1021/ma0492465.
22. Wittmann JC, Smith P. Highly oriented thin films of poly(tetrafluoroethylene) as a substrate for oriented growth of materials. Nature. 1991;352:414–7. https://doi.org/10.1038/352414a0.
23. Li Y, Zhou W, Cai X, Chen X, Liu H, Huang P, Wang X, Xu J. Guided organic crystalline nanowires by directional friction-transferred poly(tetrafluoroethylene) nanogrooves and their monolithic phototransistors. Adv Mater Technol. 2024;9:2302015. https://doi.org/10.1002/admt.202302015.
24. Kihara H, Ueda Y, Unno A, Hirai T. Fabrication and field effect transistor characteristics of well-ordered pentacene film. Mol Cryst Liq Cryst. 2004;424:195–202. https://doi.org/10.1080/15421400490506171.

25. Liu W, Liu W, Xu F, Wang C, Yang J, Jiang H, Zhu G. Thermal release transfer of organic semiconducting film for high-performance flexible organic electronics. ACS Appl Electron Mater. 2021;3:988–98. https://doi.org/10.1021/acsaelm.0c01078.
26. Yang J, Luo X, Liu S, Feng Y, Guliakova AA, Zhu G. Piezoelectric enhancement in P(VDF-TrFE) copolymer films via controlled and template-induced epitaxy. ACS Appl Mater Interfaces. 2024;16:38334–44. https://doi.org/10.1021/acsami.4c09892.
27. Damman P, Dosière M, Brunel M, Wittmann JC. Nucleation and oriented growth of aromatic crystals on friction-transferred poly(tetrafluoroethylene) layers. J Am Chem Soc. 1997;119:4633–9. https://doi.org/10.1021/ja961173k.
28. Funahashi M, Mori Y. Linearly polarized electroluminescence device in which the polarized plane can be rotated electrically using a chiral liquid crystalline semiconductor. Mater Chem Front. 2020;4:2137–48. https://doi.org/10.1039/D0QM00086H.
29. Funahashi M, Sonoda A. High electron mobility in a columnar phase of liquid-crystalline perylene tetracarboxylic bisimide bearing oligosiloxane chains. J Mater Chem. 2012;22:25190–7. https://doi.org/10.1039/C2JM35579E.
30. Liao J, Wang X, Danieli Y, Houben L, Rechav K, Song J, Song J, Zhao Z, Zhang L, Zhou G, Joselevich E, Xu J. Aligned Phthalocyanine Molecular Nanowires by Graphoepitaxial Self-Assembly and Their In Situ Integration into Photodetector Arrays. Adv Mater Technol. 2023;8:2202179. https://doi.org/10.1002/admt.202202179.
31. Jiang H, Hu P, Ye J, Ganguly R, Li Y, Long Y, Fichou D, Hu W, Kloc C. Hole mobility modulation in single-crystal metal phthalocyanines by changing the metal–π/π–π interactions. Angew Chem. 2018;130:10269–74. https://doi.org/10.1002/ange.201803363.
32. Kumar P, Sharma A, Yadav S, Ghosh S. Morphology optimization for achieving air stable and high performance organic field effect transistors. Org Electron. 2013;14:1663–72. https://doi.org/10.1016/j.orgel.2013.03.027.
33. Cranston RR, Lessard BH. Metal phthalocyanines: thin-film formation, microstructure, and physical properties- a review. RSC Adv. 2021;11:21716–37. https://doi.org/10.1039/D1RA03853B.
34. Rani V, Sharma A, Kumar P, Singh B, Ghosh S. Charge transport mechanism in copper phthalocyanine thin films with and without traps. RSC Adv. 2017;7:54911–9. https://doi.org/10.1039/C7RA08316E.
35. Chowdhury A, Biswas B, Majumder M, Sanyal MK, Mallik B. Studies on phase transformation and molecular orientation in nanostructured zinc phthalocyanine thin films annealed at different temperatures. Thin Solid Films. 2012;520:6695–704. https://doi.org/10.1016/j.tsf.2012.07.013.
36. Wojdyła M, Derkowska B, Łukasiak Z, Bała W. Absorption and photoreflectance spectroscopy of zinc phthalocyanine (ZnPc) thin films grown by thermal evaporation. Mater Lett. 2006;60:3441–6. https://doi.org/10.1016/j.matlet.2006.03.029.
37. Karan S, Mallik B. Effects of annealing on the morphology and optical property of copper (II) phthalocyanine nanostructured thin films. Solid State Commun. 2007;143:289–94. https://doi.org/10.1016/j.ssc.2007.05.043.
38. Tazhibayev S, Zeinidenov A, Rozhkova X, Zhakanova A, Aimukhanov A, Mukametkali T, Paygin V, Valiev D. Influence of the transition metals central atom nature on the optical and electrophysical properties of phthalocyanine nanowires. Mater Chem Phys. 2023;301: 127696. https://doi.org/10.1016/j.matchemphys.2023.127696.
39. Abe T, Hiyama Y, Fukui K, Sahashi K, Nagai K. Efficient p-zinc phthalocyanine/n-fullerene organic bilayer electrode for molecular hydrogen evolution induced by the full visible-light energy. Int J Hydrog Energy. 2015;40:9165–70. https://doi.org/10.1016/j.ijhydene.2015.05.155.
40. Jungyoon E, Kim S, Lim E, Lee K, Cha D, Friedman B. Effects of substrate temperature on copper(II) phthalocyanine thin films. Appl Surf Sci. 2003;205:274–9. https://doi.org/10.1016/S0169-4332(02)01115-7.
41. Davis R, Asokan AN, Predeep P. Effect of annealing induced morphology on mobility of copper phthalocyanine thin films. J Inorg Organomet Polym. 2020;30:4408–15. https://doi.org/10.1007/s10904-020-01587-6.
42. Schünemann C, Elschner C, Levin AA, Levichkova M, Riede M. Zinc phthalocyanine — influence of substrate temperature, film thickness, and kind of substrate on the morphology. Thin Solid Films. 2011;519:3939–45. https://doi.org/10.1016/j.tsf.2011.01.356.
43. Rand BP, Cheyns D, Vasseur K, Giebink NC, Mothy S, Yi Y, Coropceanu V, Beljonne D, Cornil J, Bredas J-L, Genoe J. The impact of molecular orientation on the photovoltaic properties of a phthalocyanine/fullerene heterojunction. Adv Funct Mater. 2012;22:2987–95. https://doi.org/10.1002/adfm.201200512.
44. Koshiba Y, Yamamoto M, Kinashi K, Misaki M, Ishida K, Oguchi Y, Ueda Y. Photo-induced alignment behavior of azobenzene compound in thin film. Thin Solid Films. 2009;518:805–9. https://doi.org/10.1016/j.tsf.2009.07.090.
45. Bidmeshkipour S, Akhavan O, Salami P, Yousefi L. Aperiodic perforated graphene in optical nanocavity absorbers. Mater Sci Eng B. 2022;276:115557. https://doi.org/10.1016/j.mseb.2021.115557.
46. Badán JA, Marotti RE, Dalchiele EA, Ariosa D, Martín F, Leinen D, Ochoa E, Ramos-Barrado JR. Optical properties of Si nanowires: dependence on substrate crystallographic orientation and light polarization. J Mater Res. 2015;30:753–60. https://doi.org/10.1557/jmr.2015.47.
47. Hokari R, Takakuwa K, Shiomoto K, Kuwano G, Kurihara K. Development and analysis of a nano-triangular wave-shaped polarizer. Sci Rep. 2023;13:13387. https://doi.org/10.1038/s41598-023-40511-z.
48. Fronk M, Bräuer B, Salvan G, Zhan DRT. Molecular alignment in α-CuPc films probed by reflection anisotropy spectroscopy. J Mol Struct. 2014;1073:82–6. https://doi.org/10.1016/j.molstruc.2014.05.001.
49. Yadav N, Kumari N, Ando Y, Pandey SS, Singh V. PCPDTBT copolymer based high performance organic phototransistors utilizing improved chain alignment. Opt Mater. 2021;113: 110886. https://doi.org/10.1016/j.optmat.2021.110886.
50. Ofuji M, Inaba K, Omote K, Hoshi H, Takanishi Y, Ishikawa K, Takezoe H. Growth process of vacuum deposited copper phthalocyanine thin films on rubbing-treated substrates. Jpn J Appl Phys. 2003;42:7520–4. https://doi.org/10.1143/JJAP.42.7520.
51. Shahiduzzaman M, Horikawa T, Hirayama T, Nakano M, Karakawa M, Takahashi K, Nunzi J-M, Taima T. Switchable crystal phase and orientation of evaporated zinc phthalocyanine films for efficient organic photovoltaics. J Phys Chem C. 2020;124:21338–45. https://doi.org/10.1021/acs.jpcc.0c07010.
52. Wagner SR, Zhang P. Nucleation and evolution of zinc phthalocyanine thin films on the deactivated Si(111)-B 3×3 R30° surface. Surf Sci. 2014;630:22–7. https://doi.org/10.1016/j.susc.2014.06.025.
53. Ueda Y, Kuriyama T, Hari T, Ashida M. Crystal growth and molecular orientation of organic materials vapor-deposited on highly-oriented polytetrafluoroethylene thin film. J Electron Microsc. 1994;43:99–103. https://doi.org/10.1093/oxfordjournals.jmicro.a051093.
54. Yang T, Jin C, Qu J, Darvish AA, Sabatini R, Zhang X, Chen H, Ringer SP, Lakhwani G, Li F, Cairney J, Liu X, Zheng R. Solution epitaxy of halide perovskite thin single crystals for stable transistors. ACS Appl Mater Interfaces. 2021;13:37840–8. https://doi.org/10.1021/acsami.1c08800.

55. Sitter H, Andreev A, Teichert Ch, Hlawacek G, Haber T, Smilgies D-M, Resel R, Ramil AM, Sariciftci NS. Organic thin films grown by hot wall epitaxy on inorganic substrates. Phys Status Solidi B. 2005;242:1877–82. https://doi.org/10.1002/pssb.200461752.
56. Yang CY, Yang Y, Hotta S. Crystal structure and polymorphism of dimethyl-oligothiophenes crystallized epitaxially on highly oriented PTFE thin films. Synth Met. 1995;69:303–4. https://doi.org/10.1016/0379-6779(94)02460-G.
57. van de Craats AM, Stutzmann N, Bunk O, Nielsen MM, Watson M, Müllen K, Chanzy GD, Sirringhaus H, Friend RH. Meso-epitaxial solution-growth of self-organizing discotic liquid-crystalline semiconductors. Adv Mater. 2003;15:495–9. https://doi.org/10.1002/adma.200390114.
58. Iwatsu F, Kobayashi T, Uyeda N. Solvent effects on crystal growth and transformation of zinc phthalocyanine. J Phys Chem. 1980;84:3223–30. https://doi.org/10.1021/j100461a018.
59. Senthilarasu S, Sathyamoorthy R, Kulkarni SK. Substrate temperature effects on structural orientations and optical properties of ZincPthalocyanine (ZnPc) thin films. Mater Sci Eng B. 2005;122:100–5. https://doi.org/10.1016/j.mseb.2005.05.005.
60. Hori T, Shibata T, Kittichungchit V, Moritou H, Sakai J, Kubo H, Fujii A, Ozaki M. MoO3 buffer layer effect on photovoltaic properties of interpenetrating heterojunction type organic solar cells. Thin Solid Films. 2009;518:522–5. https://doi.org/10.1016/j.tsf.2009.07.044.
61. Hasegawa J, Nagase T, Kobayashi T, Naito H. Write-once memory effects observed in Ga-doped ZnO/organic semiconductor/MoO_3/Au structures. Jpn J Appl Phys. 2016;55:03DC05. https://doi.org/10.7567/JJAP.55.03DC05.